Low-cost, high-efficiency organic/inorganic hetero-junction hybrid solar cells for next generation photovoltaic device

P R Pudasaini[1, 2] and A A Ayon[1]
[1]MEMS Research Laboratory, Department of Physics and Astronomy, The University of Texas at San Antonio
One UTSA Circle, San Antonio, Texas, 78249, USA

[2]E-mail: pbz620@my.utsa.edu

Abstract. Organic/inorganic hybrid structures are considered innovative alternatives for the next generation of low-cost photovoltaic devices because they combine advantages of the purely organic and inorganic versions. Here, we report an efficient hybrid solar cell based on sub-wavelength silicon nanotexturization in combination with the spin-coating of poly (3,4-ethylene-dioxythiophene):polystyrenesulfonate (PEDOT:PSS). The described devices were analyzed by collecting current-voltage and capacitance-voltage measurements in order to explore the organic/inorganic heterojunction properties. ALD deposited ultrathin aluminium oxide was used as a junction passivation layer between the nanotextured silicon surface and the organic polymer. The measured interface defect density of the device was observed to decrease with the inclusion of an ultrathin Al_2O_3 passivation layer leading to an improved electrical performance. This effect is thought to be ascribed to the suppression of charge recombination at the organic/inorganic interface. A maximum power conversion efficiency in excess of 10% has been achieved for the optimized geometry of the device, in spite of lacking an antireflection layer or back surface field enhancement schemes.

1. Introduction

Sun light is an abundant and renewable energy resource, and converting sunlight into electricity has been regarded as one of the most promising approaches to provide clean energy. Conventional silicon solar cells usually require high purity silicon materials and relatively complex fabrication methods, therefore, they are not necessarily cost effective for a wide range of applications. Organic photovoltaic solar cells (OPV) on the other hand, have become a promising candidate for achieving low cost solar energy conversion devices, since they can be fabricated by relatively simpler and cost-effective processing schemes, such as screen printing, ink jet printing, dip coating and roll to roll processing. Additionally, they also have the advantage of being lightweight and mechanically flexible. However, as of today, state-of-the-art organic solar cells exhibit a relatively low power conversion efficiency (*PCE)* compared to their single crystal silicon counterparts. One of the greatest challenges of OPV is the relative paucity of electron accepting materials which may be paired with hole conducting polymers to induce exciton dissociation at the interface. An interesting approach to this problem is to use semiconducting nanostructures as an electron accepting phase to form organic/inorganic hybrid solar cells [1-3]. Hybrid solar cells comprised of p-type organic polymer thin film and n-type silicon substrate have been extensively investigated in the recent development of high efficiency and cost effective solar cells device. To date, a *PCE* value as high as ~10% has been reported for hybrid

heterojunction devices, fabricated by spin coating the polymer (3,4-ethylene-dioxythiophene):polystyrenesulfonate (PEDOT:PSS) on a nanotextured silicon surface [4-7], however, it should be noted that there is a noticeable widespread in PCE values extending to the relatively low value of 1% or less [8,9]. Additionally, vertically aligned silicon nanowires (SiNWs) have been reported to exhibit excellent light absorption characteristics both theoretically and experimentally [10-12]. The quality of the interface between PEDOT:PSS and nanotextured silicon surface is believed to contribute greatly to the large discrepancy observed in the reported *PCE* values which is predicted to have a strong dependence in several variables, namely, the conductivity and wettability of PEDOT:PSS, the spin coating parameters (spin casting speed and time) employed to control the thickness of the PEDOT:PSS layer on the textured silicon surface, and the annealing temperature after the spin coating process, that could all influence the interface properties of a hybrid solar cell. A thin dielectric interface passivation layer between silicon and PEDOT:PSS layer could also have a significant effect on the electrical performance of the proposed hybrid devices. Different groups have employed a variety of dielectric materials as a junction passivation layer (i.e., recombination barrier) for the proposed PEDOT:PSS/Silicon hybrid solar cells and reported the enhanced electrical performance of the device. He *et al.* [13] and Zhang *et al.* [14] independently reported that a thin native oxide (SiOx) is crucial for the enhanced photovoltaic performance of the device compared to the H-terminated silicon surface. This can be attributed to the formation of a favorable internal electric field at the interface for an efficacious carrier extraction. In this letter, we report an efficient hybrid solar cell composed of vertically aligned silicon nanostructured arrays and PEDOT:PSS organic polymer employing an ultra-thin ALD deposited Al_2O_3 junction passivation layer.

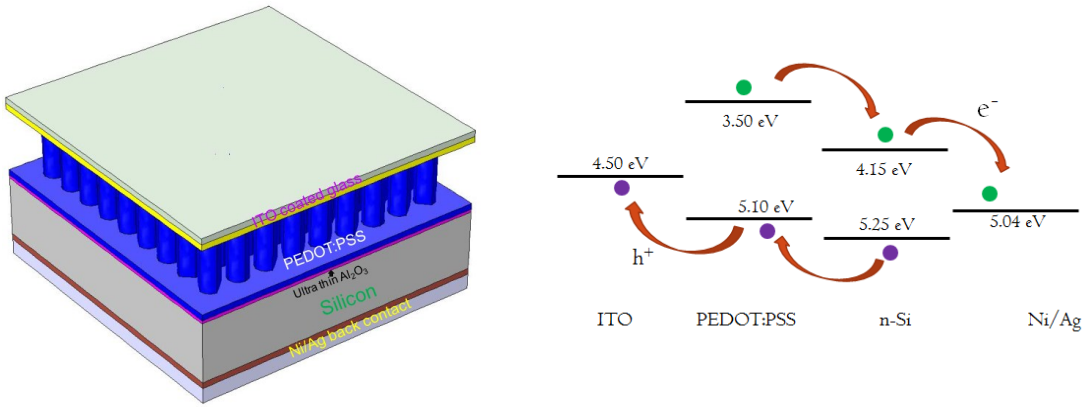

Figure 1. Schematic illustration of the fabricated Silicon/PEDOT:PSS solar cell (left), energy band diagram of the described hybrid solar cell (right).

2. Experimental Section

Highly ordered wafer-scale silicon nanopillar (SiNPs) array textured surfaces were fabricated by metal assisted electroless chemical etching in combination with nanosphere lithography. The detailed fabrication procedure can be found elsewhere [15-17]. The ALD of Al_2O_3 was carried out with a Cambridge Nanotech Savanah 200 system. The platen temperature was maintained at 110ºC during the deposition process. The precursors, trimethylaluminium (TMA) and water (H_2O) were kept at room temperature. Nitrogen (N_2) was employed as a carrier and purging gas. ALD is a deposition process that employs cyclical self-limiting gas-surface reactions, and this property is important for a conformal deposition on high aspect ratio structures due to the time required for the reactant gases to fully diffuse into the narrow channel. Prior to device fabrication, the produced textured silicon samples were cleaned with a modified RCA procedure. After native-oxide removal the samples were transferred to the ALD chamber for a ~7A° Al_2O_3 deposition. Subsequently, 10 nm of nickel and 400

nm of silver were deposited on the back side and the samples were annealed at 425˚C for 30 min to form a rear ohmic contact. Highly conductive PEDOT:PSS (Sigma-Aldrich) mixed with dimethyl sulphoxide and Triton X-100 (surfactant) solution was spin cast at 300 rpm for 10 s and 2000 rpm for 60 s to form a core-shell radial junction. The samples were then annealed on a hotplate at 140°C for 10 min to remove the solvent. Finally, an ITO coated glass with a resistivity of 8-12 Ω/sq (Sigma-Aldrich) was employed as a front contact to complete the solar cell. Each device had an active area of 1 cm^2. Figure 1 depicts the schematic illustration of the fabrication of a SiNPs/PEDOT:PSS solar cell. The morphology of the samples was collected by using high-resolution scanning electron microscopy (SEM) with a Field emission gun Hitachi S-5500. The PV measurement was performed using a solar simulator (Newport Sol2A) under AM 1.5G illumination (1000W/m^2) at standard testing conditions. Prior to each sample measurement, the simulator intensity was calibrated with a reference solar cell from Newport (Irvine CA, USA) to ensure that the irradiation variation was within 3%.

3. Results and discussion

Figure 2 includes a large SEM micrograph of the vertically aligned nanopillar array (top view) fabricated by the aforementioned metal assisted electroless chemical etching method. The same Figure 2 includes an inset in the upper right corner with higher magnification SEM micrographs of the same sample. Nanosphere lithography was employed to control the dimension of the SiNPs (diameter and inter-pillar spacing). The distance between the centers of any two pillars was fixed at 650 nm, and this value was determined by using Polystyrene nanoparticles with that particular diameter. The density of the SiNPs array was measured to be ~2.7×10^6 pillars/mm^2. The inset in the lower left corner in Figure 2 shows the top view of PEDOT:PSS coated SiNPs array textured surface. The thickness of the PEDOT:PSS layer was approximately 40 nm. SiNPs arrays with average heights of 200 nm, 400 nm, 800 nm, and 1200 nm were fabricated by etching the sample for 30 s, 60 s, 120 s, and 180 s, respectively. The height of the SiNPs plays an important role in device performance. The current-voltage characteristics of the SiNPs/PEDOT:PSS hybrid solar cells having different nanopillar heights were measured under 100 mW/cm^2 illumination. Figure 3 depicts the average value of short circuit current density (J_{SC}), open circuit voltage (V_{OC}), fill factor (*FF*) and power conversion efficiency (*PCE*) of the fabricated devices as a function of SiNPs height. The measured value of short circuit current density for the fabricated SiNPs/PEDOT:PSS solar cells, increases as the nanopillar height increases, reaches a maximum of 29.5 mA/cm^2 for a SiNPs height of 0.4 μm (see Figure 3a), beyond this particular point, it decreases quasi-linearly to 21.2 mA/cm^2 as the height is further increased to 1.2 μm. Similar effects have also been reported elsewhere [5,18]. The remarkable antireflection property of the SiNPs array textured surface is directly reflected in the measured value of J_{SC} of the SiNPs/PEDOT:PSS solar cell. The maximum J_{SC} of 29.5 mA/cm^2 for a SiNPs array textured cell with SiNPs height of 0.4 μm is almost 36.6% greater than a planar/PEDOT:PSS cell. On the other hand, the measured open circuit voltage of the SiNPs/PEDOT:PSS solar cells was observed to decrease continuously from a maximum value of 538 mV to a minimum of 490 mV as the SiNPs height varied from 0.2 μm to 1.2 μm (see Figure 3a). This can be attributed to an increased junction recombination with increases in surface area. The power conversion efficiency of the SiNPs/PEDOT:PSS solar cells produced, reached a maximum value of 9.65%, for a nanopillar height of 0.4 μm, which compares favorably to the 7.02% observed for a planar/PEDOT:PSS cell. This is mainly due to the increase in short circuit current density and fill factor for the device, despite the slight decrease in V_{OC}. A promising fill factor value of 62 was achieved for a SiNPs/PEDOT:PSS hybrid cell which also compares favorably to *FF* of 60 for a planar/PEDOT:PSS solar cell. This could be attributed to an increased carrier separation due to the increased junction area. Furthermore, the SiNPs/PEDOT:PSS heterojunction provides a shorter pathway for the minority charge carriers towards the respective electrode. One factor limiting the efficiency of SiNPs/PEDOT:PSS hybrid cells is the low carrier collection efficiency due to increased surface recombination, in spite of having better light absorption

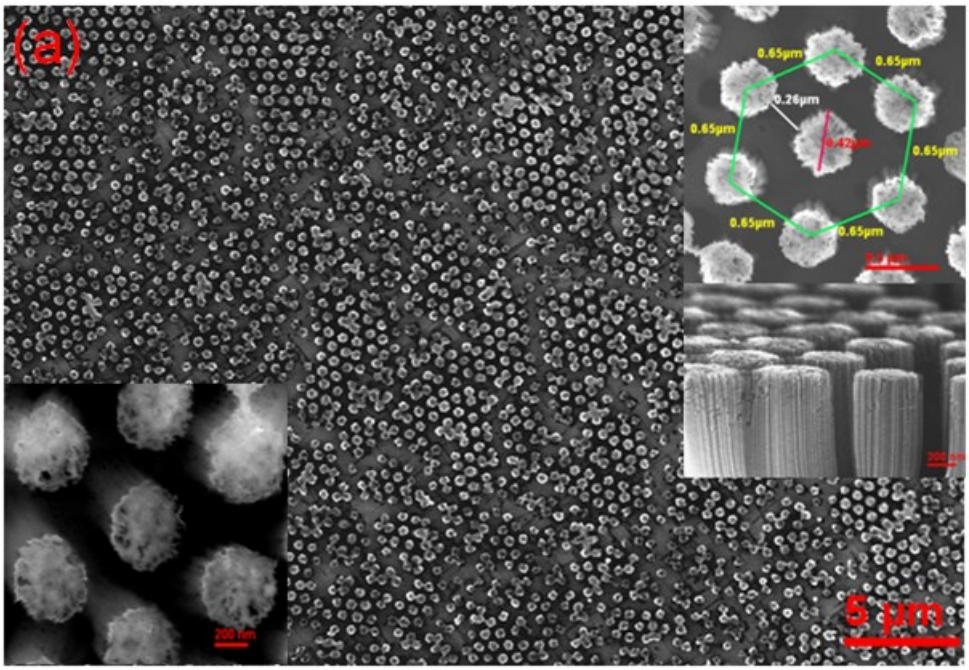

Figure 2. SEM micrographs of top view of a SiNP array textured silicon surface; the inset on the upper right corner includes higher magnification images of the same sample, where it is possible to discern the hexagonal order of the SiNPs array. The inset on the lower left corner shows a high magnification image of the SiNPs array, coated with the transparent and conductive polymer PEDOT:PSS by spin casting at 2000 rpm.

characteristics. The open circuit voltage of a SiNPs/PEDOT:PSS solar cells, irrespective of pillar height, is observed to be smaller compared to their planar/PEDOT:PSS counterparts.To reduce the recombination at the nanotextured silicon surface with a SiNPs/PEDOT:PSS structure we employed an ultrathin (~0.7 nm) ALD Al_2O_3 as an interface passivation layer. ALD Al_2O_3 was chosen as a passivation layer due to its unique chemical and field effect passivation characteristics, as well as the ability of ALD to deposit high quality, conformal films on high aspect ratio features, with an angstrom-level control of film thickness at low temperatures. The height of the SiNPs was fixed at 0.4 μm. It was found that the power conversion efficiency of the devices increased with the utilization of Al_2O_3 interface layer, with a maximum value of 10.56%, while the *PCE* of the same device without Al_2O_3 was 9.65%. This can be attributed mainly to the increased open circuit voltage of the device. The maximum open circuit voltage of 578 mV was achieved with an interfacial ALD Al_2O_3, which is ~9.1% higher compared to the same device without Al_2O_3 interface layer. The maximum short circuit current density of the cell with the Al_2O_3 barrier layer was 30.1 mA/cm^2 compared to 29.5 mA/cm^2 for a cell without Al_2O_3 despite the slight decrease in *FF*. To investigate the underlying reasons for the observed voltage gain, we measured and graphed the dark current density versus voltage characteristics of the hybrid SiNPs/PEDOT:PSS solar cells with and without Al_2O_3 interface layer. The observations indicate that the dark current density is suppressed significantly after employing the ultrathin Al_2O_3 barrier layer (see figure 4 a) (see Figure 4(a)). From the best fitting of the dark *J-V* characteristic curves at the forward bias condition, we extracted the values of saturation current density (J_o) and diode ideality factor (n) of the described device. We obtained the value of J_o to be 0.48 μA/cm^2 for a SiNPs/PEDOT:PSS hybrid cell with an Al_2O_3 barrier layer, which was lower than that of a cell without a barrier layer, namely, 2.19 μA/cm^2.

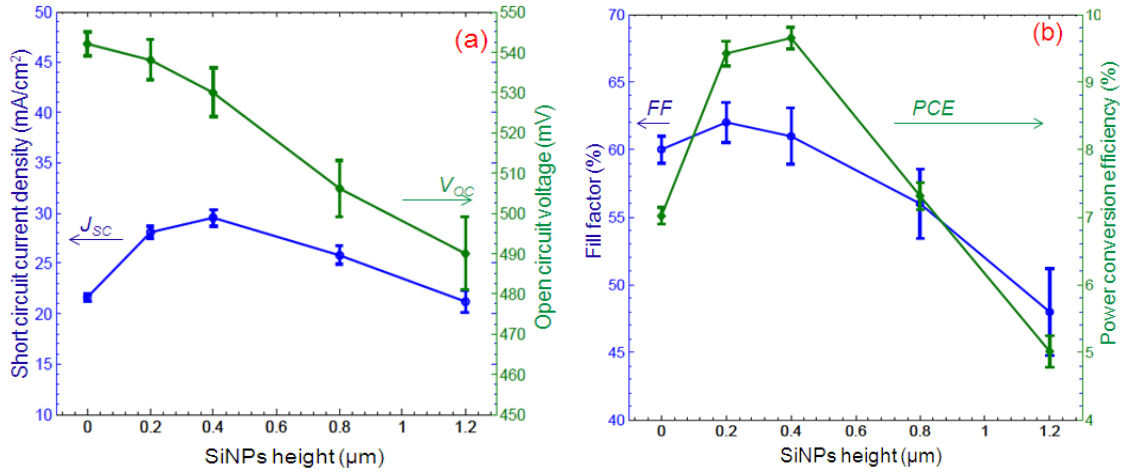

Figure 3. Average photovoltaic performance parameters of (a) *Jsc* and *Voc* and (b) *FF* and *PCE* of the SiNPs/PEDOT:PSS solar cell as a function of SiNPs height.

The ideality factors of 2.06 and 2.21, respectively, were obtained for the SiNPs/PEDOT:PSS cells with and without the Al_2O_3 barrier layer.

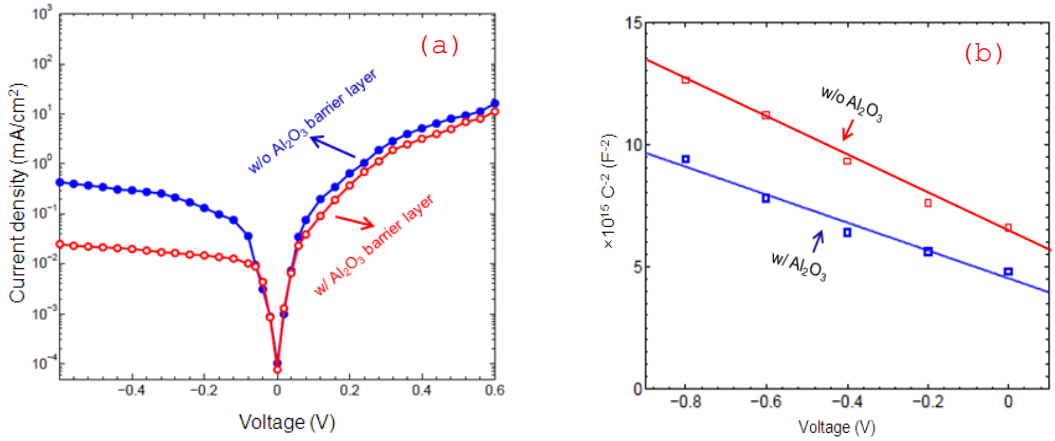

Figure 4. The dark *J-V* characteristics curve (a), C^{-2}-*V* plots (b), for SiNPs/PEDOT:PSS solar cells with and without Al_2O_3 passivation layer.

We also performed the capacitance voltage (*C-V*) measurements for the devices with and without Al_2O_3 passivation layers. Neglecting the series resistance of the devices, the interfacial defect density arising from the presence of chemical defects, such as dangling bonds, nonconformal coating of organic polymer etc., can be calculated by using the equations below.

$$\left(\frac{1}{C^2}\right) = \frac{2}{c_2{}^2 q\varepsilon N_A}\left(\Phi_B - c_2 V - \nu_p\right) \tag{1}$$

$$c_2 = \frac{\varepsilon_0}{\varepsilon_0 + q^2 \delta D_{it}} \tag{2}$$

where, Φ_B is the barrier height, V is the applied voltage, v_p is the difference between the Si Fermi level and valence band, N_A is the doping concentration, δ is the interface thickness, D_{it} is the interfacial defect density and ε_0 and ε are the permittivity of vacuum and silicon respectively. Figure 4(b) depicts the C^{-2} versus V plot for the optimized SiNPs/PEODT:PSS solar cells with and without interfacial Al_2O_3 passivation layer. Ostensibly, the C^{-2}-V plot is linear and we extracted the value of interfacial defect density of the devices from the slope of the corresponding C-^{2}-V plot. For the device with the Al_2O_3 passivation layer, the D_{it} value of 2.80×10^{12} $cm^{-2}eV^{-1}$ was achieved while for the device without passivation layer a significantly higher value of 4.16×10^{12} $cm^{-2}eV^{-1}$ was obtained. The reduced interfacial defect density was responsible for the lower saturation current density and hence the improved open circuit voltage and power conversion efficiency of the device.

4. Conclusions

We have employed a relatively simple and wafer scalable process to produce and characterize a heterojunction PEDOT:PSSs/SiNP hybrid solar cell that could prove useful in the quest of low-cost yet efficient photovoltaic devices. The effect of SiNP height on solar cell performance was investigated. The *PCE* of a SiNPs/PEDOT:PSS hybrid cell with an optimized SiNPs height of 0.4 μm was observed to be 9.65%. With the utilization of an ultrathin ALD deposited Al_2O_3 junction passivation layer, we observed a short circuit current density and an open circuit voltage as high as 30.1 mA/cm^2 and 578 mV respectively, which led to a *PCE* value in excess of 10.56%. The described hybrid device was formed by spin coating the organic polymer PEDOT:PSS on SiNPs arrays fabricated by relatively simple, low-cost, room temperature methods, which could lead to the proliferation of low cost photovoltaic devices in the future.

Acknowledgement

We thank Dr. Mike Gerhold, Technical Manager of the U.S. Army Research Office, for the financial support provided for this project (ARO grant number W911NF-13-1-0110).

References

[1] Lin C Y, Holman Z C and Kortshagen U R 2009 *Nano Letts.* **9** 449
[2] He L, Jiang C, Rusli, Lai D and Wang H 2011 *Appl. Phys. Letts*. **99** 021104
[3] Huynh W U, Dittmer J J and Alivisatos A P 2002 *Science* **295** 2425
[4] Avasthi S, Lee S, Loo Y L and Sturm J C 2011 *Adv. mater.* **23** 5762
[5] He L, Jiang C, Wang H, Lai D and Rusli 2012 *ACS appl. mater. interfaces* **4** 1704
[6] Jeong S, Garnett E C, Wang S, Yu Z, Fan S, Brongersma M L, McGehee M D and Cui Y 2012 *Nano letts.* **12** 2971
[7] Khatri I, Tang Z, Liu Q, Ishikawa R, Ueno K and Shirai H 2013 *Appl. Phys. Letts.* **102** 063508
[8] Lu W, Wang C, Yue W and Chen L 2011 *Nanoscale* **3** 3631
[9] Moiz S A, Nahhas A M, Um H D, Jee S W, Cho H K, Kim S W and Lee J H 2012 *Nanotechnol.* **23** 145401
[10] Han S E and Chen G 2010 *Nano letts.* **10** 1012
[11] Pudasaini P R, Elam D and Ayon A A 2013 *J. Phys. D: Appl. Phys.* **46** 235104
[12] Pudasaini P R, and Ayon A A 2013 *Microsyst. Technol.* **19** 871
[13] He L, Jiang C, Wang H, Lai D and Rusli 2012 *Appl. Phys. Letts.* **100** 073503
[14] Zhang F, Sun B, Song T, Zhu X and Lee S 2011 *Chem. Mater.* **23** 2084
[15] Mikhael B, Elise B, Xavier M, Sebastian S, Johann M and Laetitia P 2011 *ACS appl. mater. interfaces* **3** 3866
[16] Pudasaini P R and Ayon A A 2013 *Microelect. Eng*. **110** 126
[17] Huang Z, Geyer N, Werner P, Boor J and Gosele U 2011 *Adv. mater.* **23** 285
[18] Syu H J, Shiu S C and Lin C F 2012 *Sol. Energy Mater. Sol. Cells* **98** 267